

## PULSED LASER ABLATION METHOD FOR PRODUCTION OF Zn-Ag ALLOY NANOPARTICLES

M. A. AHMED<sup>a\*</sup> , W. Y. Khudhair<sup>a</sup>,

<sup>a</sup> Iraqi Ministry of Education, Diyala, Iraq.

\*m2amaiss@gmail.com

### Abstract :

In the past ten years, researchers have become interested in a contemporary and effective technique called pulsed laser ablation of a metallic target in liquid (PLAL). Bimetallic liquid colloidal (Zn/Ag) alloy nanoparticles were produced using the pulsed laser ablation in liquids (PLAL) technique, excised in liquid sodium dodecyl sulfate (SDS) (5mM and 10mM SDS), and then put through morphological (TEM), optical (UV-VIS), and structure (FTIR) studies. The (TEM) test findings showed that the (NPs) are spherical and semi-spherical in shape, and they also showed that the absorption spectra showed the peak value of surface plasmon resonance (SPR), which was (410 and 408) nm for the (Cu/ Ag) alloy formed in solution (SDS) correspondingly. Following FTIR analysis, it was discovered that the following effective groups were present in the product samples: (O-H, C-H, C-O, Ag-O and Zn-O).

**Keywords:** Zn-Ag, Alloy, Nanoparticles, SDS, Laser Ablation, TEM, UV-VIS, FTIR.

### طريقة الاستئصال بالليزر النبضي

### لإنتاج سبائك (الخاصين- فضة) النانوية في SDS

ميس اديب احمد\* ، وسام ياس خضير

وزارة التربية العراقية، العراق، ديالى

m2amaiss@gmail.com\*

### مستخلص:

في السنوات العشر الماضية، أصبح الباحثون مهتمين بتقنية معاصرة وفعالة تسمى الاستئصال بالليزر النبضي لهدف معدني في سائل (PLAL). تم في هذه الدراسة إنتاج الجسيمات النانوية السائلة الغروانية ثنائية المعدن (Zn/Ag) باستخدام تقنية الاستئصال بالليزر النبضي في السوائل (PLAL)، وجرى استئصالها في كبريتات دوديسيل الصوديوم السائلة ((5مل و10) مل، من ثم تشخيصها من خلال الشكل المورفولوجي (TEM)، الفحص البصري (UV-VIS) والدراسات التركيبية (FTIR)، وقد أظهرت نتائج اختبار (TEM) أن الجسيمات النانوية (NPs) كروية وشبه كروية الشكل، كما بينت أن أطراف الامتصاص أظهرت أعلى قيمة لرنين البلازمون السطحي (SPR)، والتي كانت (410 و 408) نانومتر. سبيكة (Cu / Ag) المتكونة في محلول (SDS) في المقابل. بعد تحليل FTIR، تم اكتشاف أن المجموعات الفعالة التالية كانت موجودة في العينات المنتجة: (O-H، C-H، C-O، Ag-O، Zn-O). الكلمات المفتاحية: سبائك زنك-فضة، جسيمات نانوية، كبريتات دوديسيل الصوديوم، المجهر الإلكتروني النافذ، طيف الامتصاص البصري، تحويل فورييه الطيفي بالأشعة تحت الحمراء.

## 1. Introduction

Bimetallic nanoparticles, which are composed of two distinct metals, have received more scientific and technological attention than monometallic nanoparticles. The constituent metals and the nanometric size of bimetallic nanoparticles define their properties. These are produced by combining various architectural shapes of nanoparticles of metallic material. They have the capacity to enhance the energy of the metallic mixes' absorption band, producing a flexible biosensing device. Size-dependent optical, electrical, thermal, and catalytic effects are some examples of these characteristics that can differ from those of pure elemental particles [1]. Bimetallic nanoparticles can have their composition, atomic arrangement, shape, and size altered to alter their characteristics. Due to their superior optical and optoelectronic properties compared to individual/pure metals, bimetallic/alloy nanoparticles (NPs) have gained interest in a number of fields over the past ten years, including Photonics, which catalytic processes, solar cell information storage, and surface-enhanced Raman

scattering/spectroscopy (SERS) [2-7]. A quick, easy, non-catalyzed approach for creating pure colloidal metal NPs is (PLAL). It involves ablating a metal item submerged in liquid using strong laser radiation. Laser characteristics, including the wavelength of the laser, pulsing duration, and rate of repetition has an impact on the productivity and the particle size of the created NPs. During the synthesis process, a number of experimental parameters can affect the size, shape, crystallinity, and composition of NPs [8]. In general, laser ablation processes that involve one or more steps can be used to create alloy nanoparticles, such as i) laser ablation of a bulk alloy target that is submerged in a liquid, ii) laser irradiation of a metal target while it is immersed in precursor solutions ( $\text{HAuCl}_4/\text{AgNO}_3$ ), or iii) laser irradiation of individually prepared colloidal mixtures.

## 2. EXPERIMENTAL DETAILS

### 2.1 Alloy Nanoparticles synthesized by pulsed Laser Ablation.

The materials used as targets for the ablation process were highly pure Zn and Ag plates. The target was cleaned using acetone as solvent and

washed with ethanol and distilled water in an ultrasonic bath for 15 minutes to remove organic pollutants. In all the experiments, the level of the solution was 2 mm above the target surface. The nanostructures (Zn/Ag) alloy was prepared at ( $\lambda=1064\text{nm}$ ,  $f= 2\text{Hz}$ ,  $E=300\text{J}$ ) where by the sodium dodecyl sulfate (SDS) solution (5mM and

10mM) was added to a glass bottom holding a silver target, and the glass bottom was then subjected to 500 laser pulses. Next, after putting the zinc target within the colloidal Ag solution, we shot a laser at it (500 pulses). A (Zn/Ag) alloy nanostructure will also be obtained. Figure 1 shows the schematic diagram of the PLAL system.

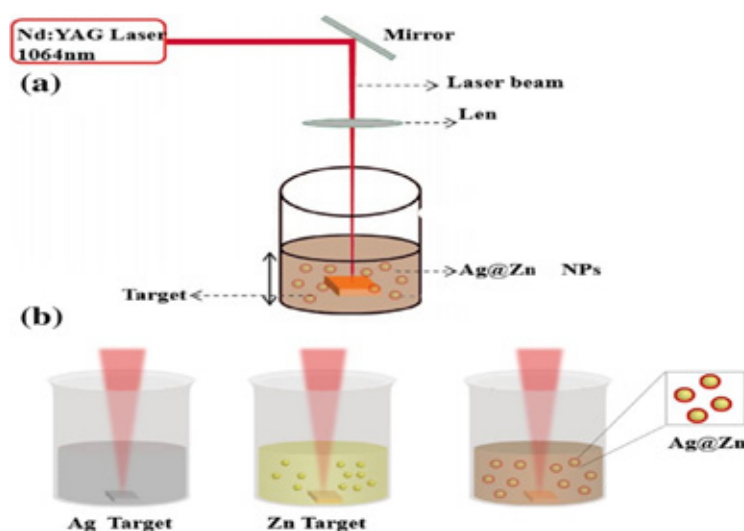


Fig.1 Schematic diagram of PLA system.

## 2.2 Characterization Techniques

The surface plasmon resonance (SPR) and absorption spectra of the colloids were recorded using (UV-Vis) spectroscopy type (Double Beam 1800 UV Spectrometer), which were used to study the structural characteristics of Au nanoparticles (Shimadzu, Japan). The spectrum was measured in a quartz cell with a (1 cm) optical path at room temperature.

## 3. RESULTS AND DISCUSSIONS

### TEM Analysis

As expected, nanoparticles of Ag and Zn in SDS solution were successfully synthesized spherically sequentially due to the mechanism of ablation in PLAL technique. And it was examined using TEM, which distributes the surface morphology and size, as well as the particle distribution and shape,

which were made clearer by TEM investigation. By comprehending the mechanism of nanoparticle generation during laser ablation in the liquid using a nanosecond laser, it is possible to explain why surfactants reduced the size of NPs, as shown by our studies. Its adiabatic expansion causes the plume to condense and cool, which causes the plasma plume species to form by collisional sticking and aggregation and then disperse in the liquid medi-

um to serve as nucleation sites for the new nanoparticle species via diffusion. Therefore, if there are surfactants in the solution, they can adsorb and cover the current nanoparticles, blocking the creation of new nanoparticles. [9,10]. This indicates that when the cavitation bubbles burst, more nanoparticle growth is possible. The TEM pictures of samples of colloidal metal nanoparticles are shown in Figure 2.

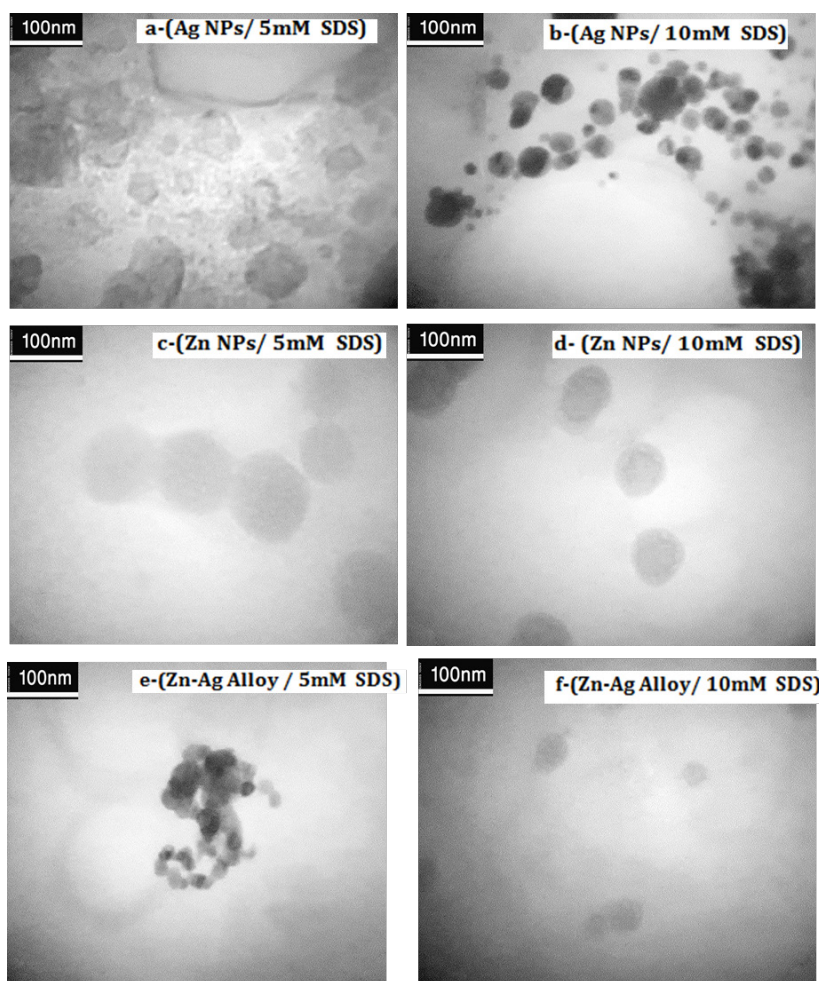


Fig. 2. TEM images of colloidal metal nanoparticles samples.

## UV-VIS Analysis and Energy Gap Calculation

Figure (3) shows the optical spectrum of absorption of alloyed Ag, Zn, and Zn/Ag NPs created by a picosecond laser in SDS solution. Ag and Zn, two distinct substances, helped to create the Ag-Zn spectrum. The spectrum of Ag nanoparticles has two peaks. Surface plasmon resonance creates the second peak, a strong transition peak at 410 nm, whereas inter-band transition creates the first peak, a modest absorption peak in the 280–290 nm region. Although the Zn absorption spectrum, which can be separated into two regions—the UV area and the visible region—has a larger absorption rate than the other spectrum in the illustration. Upon reaching the visible zone, the UV region's absorption rate dramatically declines. Figure (4) depicts the absorption spectra of Ag-Zn, which exhibit a significant peak in the UV range that is practically exact to the Zn band. Because pure Ag has a high peak at this wavelength of about 400 nm, the second peak that appears in the visible range is produced by the surface plasmon resonance of the Ag nanoparticles and is due to the presence of zinc. The

ratio of ablated Ag and Zn nanoparticles in the solution determines the general form of Ag-Zn nanoparticle optical absorption spectra. For instance, the surface plasmon resonance (SPR) peak will arise when the number of ablated Ag nanoparticles is increased, indicating a rise in the concentration of Ag in the solution. Yet when the Zn nanoparticle concentration rises, a sharp peak at 200–250 nm emerges. Long-term irradiation increased the number of ablated nanoparticles in the solution, whereas the (SPR) peak vanished as a result of nanoparticle aggregation and accumulation, which increased their weight and caused them to sink to the bottom of the solution, [12] and a shift in the absorption spectrum suggests particles in coated Zn may be smaller than the excitons' Bohr radius [13]. Figure (5) demonstrates that the shrinkage of the nanoparticle size as a result of quantitative confinement is what causes the produced nanoparticles' optical energy gap to drop in solution (SDS). Hence, obtaining tiny size particles is ideal for the bigger energy gap value [14,15].

Table 1. Absorption, surface Plasmon resonance and energy gap values of Ag, Zn and Zn/Ag alloy nanoparticles.

Nanoparticles Types	Solvent	Surface Plasmon Resonance SPR(nm)	$E_g$ (e V)
Ag NPs	5mM SDS	290, 410	2.71
	10mM SDS	290,408	2.65
Zn NPs	5mM SDS	289	2.38
	10mM SDS	289	2.5
Zn/ Ag alloy	5mM SDS	291,402	3.03
	10mM SDS	290	2.92

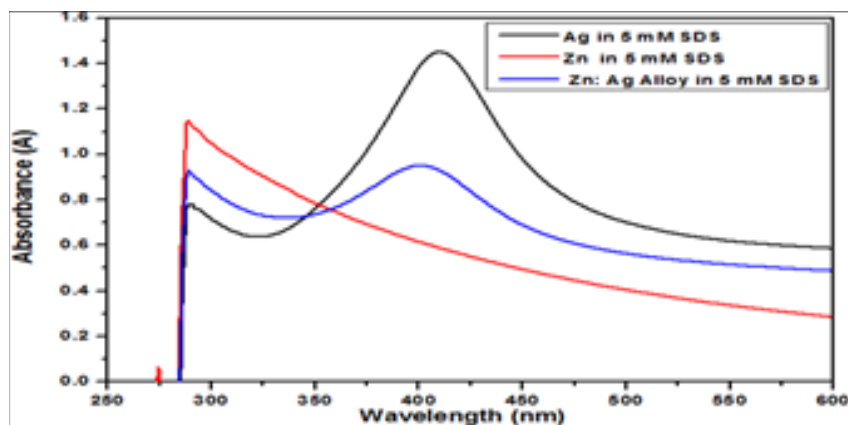
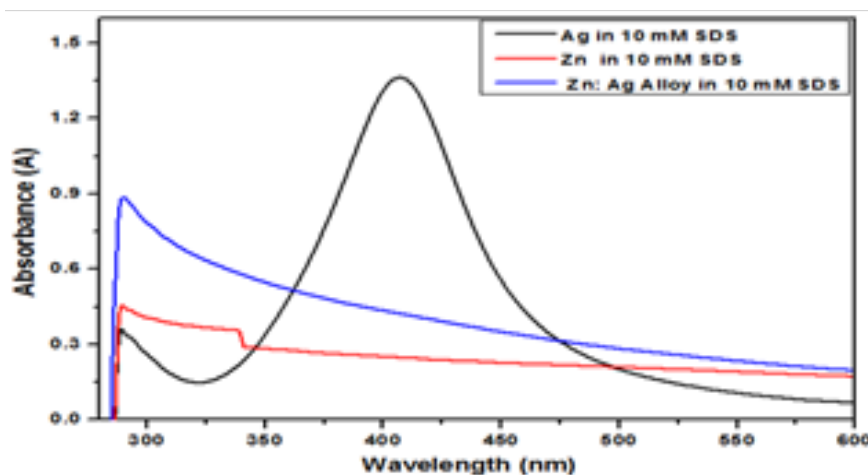


Fig. 3. UV-Visible absorption spectra of colloidal nanoparticles.

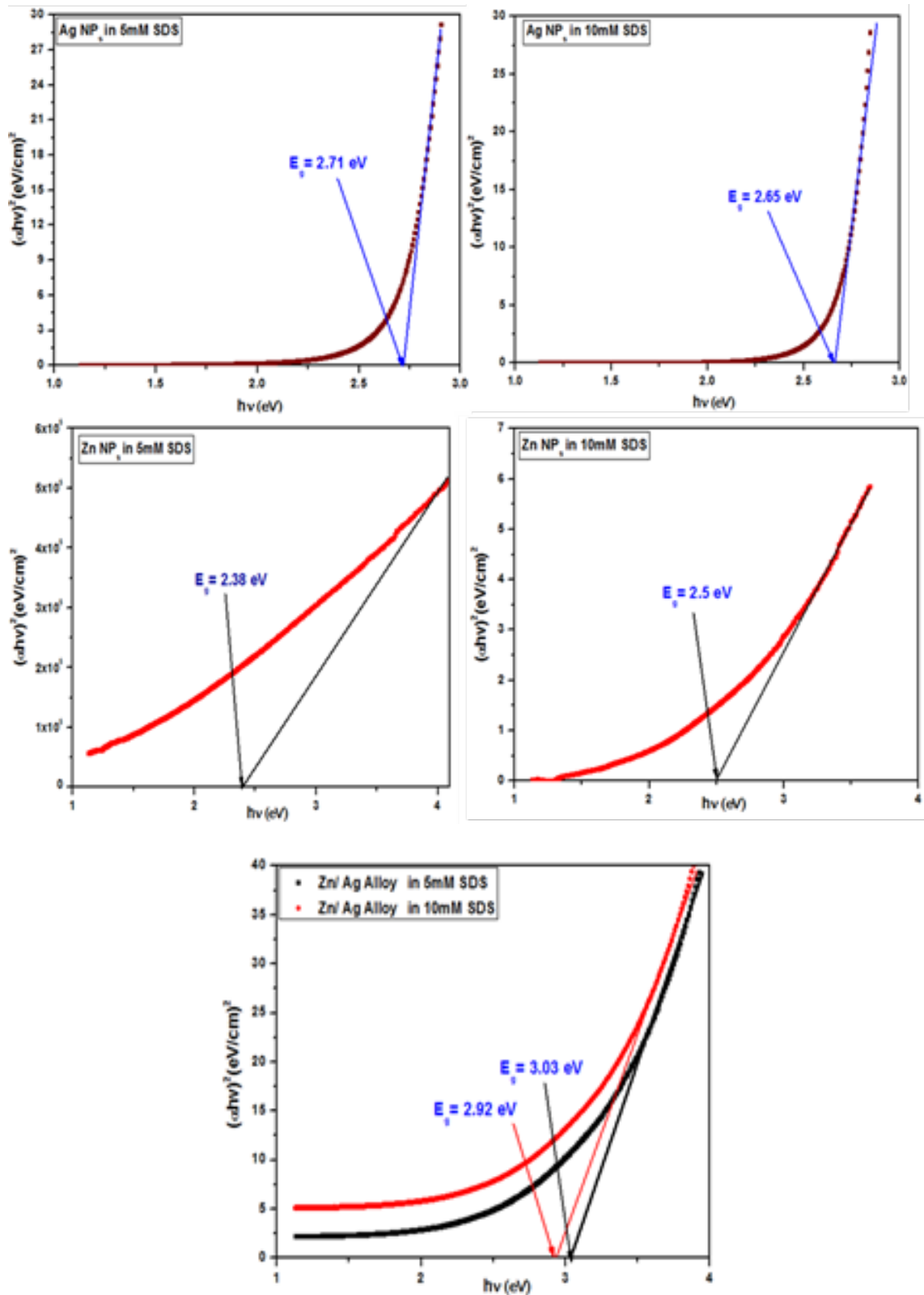


Fig. 5. Direct band gap estimations of colloidal nanoparticle samples.

### FTIR Analysis

Figures (6,7) illustrates the presence of four distinct bands in the FTIR spectrum of samples prepared for (Ag, Zn and Zn/Ag) nanoparticles in different concentration of SDS , as it was discovered that there is a strong absorption peak at (3448.4)  $\text{cm}^{-1}$  caused by vibrations of the hydroxyl group (O-H) [16], and peak at (2860.4, 2926)  $\text{cm}^{-1}$  refers to the bond  $\text{CH}_3$  while the expansion at the wave number (2092.7, 2098.5  $\text{cm}^{-1}$ ) refers to the alkene in the bond (C-H) , while it refers to the aliphatic amines (C-O) the vibrations are stretched at the

wave number (1635  $\text{cm}^{-1}$ , 1629.8  $\text{cm}^{-1}$ ), indicating an expansion pattern of the total carbon  $\text{CO}_3$  bound to the metal surface and bound to the compounds. While we also see the emergence of a peak at (1276.8 $\text{cm}^{-1}$ ) for samples made (SDS) solution, demonstrating the bond of symmetry and CH- asymmetry, where it suggests vibrations of the  $\text{CH}_3\text{-N}^+$  portion, moiety indicating that (SDS) is capped onto NPs via their head group [17,18]. Also, in both figures the band which below (582  $\text{cm}^{-1}$ ) is in charge of the Ag and Zn NPs forming and its oxides [19].

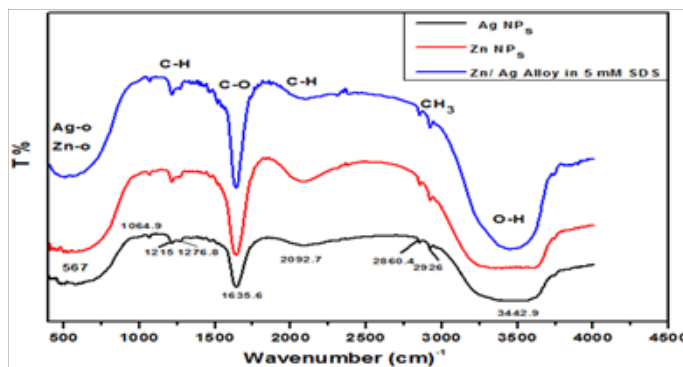


Fig. 6. FTIR spectrums of nanoparticles prepared in SDS.

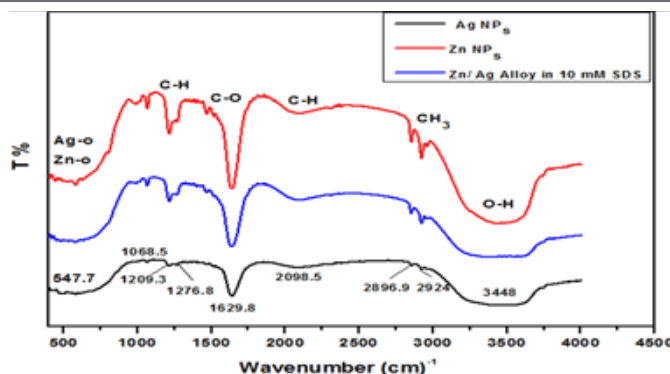


Fig. 7. FTIR spectrums of nanoparticles prepared in SDS.

#### 4. Conclusions

In conclusion, Ag/Zn nanocomposite was successfully synthesized using a simple and efficient method based on the laser ablation (Nd: YAG, 1064nm, 300 mJ and 2Hz) of Ag and Zn plates immersed in the solution from SDS. The results of the present comprehensive investigation are as follows:

1. Zn-Ag alloy NPs were made utilizing the first subsequent laser ablation process. The development of alloy NPs is indicated by the solitary SPR peak from the Zn/Ag alloy NPs' UV-visible absorption spectra that can be seen between pure NPs. The locations of these absorption peaks indicate the particle size, shape, and composition of the prepared samples.
2. UV-Vis absorption spectra and TEM pictures clearly showed the formation of homogenous alloyed particles. Where The increase in the energy gap of colloidal Zn/Ag alloy NPs could be due to the decreased size of the ablated particles as a result of the quantum size effect.
3. FTIR analysis was performed, and it was discovered that the produced samples include the effective groups

(O-H, C-H, C-O, Zn-O, and Ag O), as well as bending and stretching vibrations brought on by the presence of SDS.

#### References

- [1] G. Sharma, A. Kumar, SH. Sharma, M. Naushad, R. P. Dwivedi, Z. A. Alothman and G. T. Mola, "Novel Development of Nanoparticles to Bimetallic Nanoparticles and Their Composites", Journal of King Saud University – Science, Vol. 31, pp.257–269, (2019).
- [2] K. Chen, X. Zhang, Y. Zhang, D. Y. Lei, H. Li, T. Williams and D. R M. Farlane, "Highly Ordered Ag/Cu Hybrid Nanostructure Arrays For Ultrasensitive. Surface-Enhanced Raman Spectroscopy", Advanced Materials Interfaces, Vol. 3, pp. 1-7, (2016).
- [3] Y. Tao, M. Li, J. Ren and X. Qu, "Metal Nanoclusters: Novel Probes for Diagnostic and Therapeutic Applications", Chemical Society Reviews, Vol. 44, pp. 8636–8663, (2015).
- [4] Y. Wei, Y. Y. Zhu and M. L. Wang, "A Facile Surface-Enhanced Raman Spectroscopy Detection of Pes-

- ticide Residues with Au Nanoparticles/Dragonfly Wing Arrays”, *Optik*, Vol. 127, pp. 10735–10739, (2016).
- [5] A. Guerrero-Martínez, S. Barbosa, I. Pastoriza-Santos and L. M. Liz-Marzán, Nanostars shine bright for you: Colloidal synthesis, properties and applications of branched metallic nanoparticles, *Current Opinion in Colloid & Interface Science*, Vol. 16, pp. 118–127, (2011).
- [6] J. Zhang, M. Chaker and D. Ma, Pulsed laser ablation based synthesis of colloidal metal nanoparticles for catalytic applications, *Journal of colloid and interface science*, Vol. 489, 1pp. 38–149, (2017).
- [7] M. S. S. Bharati, B. Chandu and S. V. Rao, “Explosives sensing using Ag–Cu alloy nanoparticles synthesized by femtosecond laser ablation and irradiation”, *The Royal Society of Chemistry*, Vol. 9, pp. 1517–1525, (2019).
- [8] K. S. Tan and K. Y. Cheong, *J. Nanopart. Res.*, 2013, 15, 1537.
- [9] C. Byram and V. R. Soma, *Nano-Struct. Nano-Objects*, 2017, 12, 121–129.
- [10] M. A. Bahri, M. Hoebeke, A. Grammenos, L. Delanaye, N. Vandewalle and A. Seret, “Investigation of SDS, DTAB and CTAB Micelle Microviscosities by Electron Spin Resonance”, *Colloids and Surfaces A: Physicochemical and Engineering Aspects*, Vol. 290, pp. 206-212, (2006).
- [11] I. A. Suha, K. M. Adel and F. Zainab, “Study the Effect of Different Surfactant Solution on the Production of Zirconia (ZrO<sub>2</sub>) Nanoparticles Synthesized by Laser Ablation”, *Journal of Materials Science and Engineering*, Vol. 3, pp. 364-368, (2013).
- [12] A. H. Hamad, *Picosecond Laser Generation and Modification of Ag-TiO<sub>2</sub> Nanoparticles for Antibacterial Application*, the University of Manchester (PhD), (2016).
- [13] Ayman M. Mostafa, Eman. A. Mwafy, Ahmed M. Khalil, Arafat Toghan and Emad A. Alashkar, “ZnO/Ag multilayer for enhancing the catalytic activity against 4-nitrophenol”, *J Mater Sci: Mater Electron*, Vol.34, pp.1-9, (2023).
- [14] S. Dagher, Y. Haik, A. I. Ayeshe and N. Tit, “Synthesis and Optical Properties of Colloidal CuO

- Nanoparticles”, *Journal of Luminescence*, Vol. 151, pp.149-154, (2014).
- [15] Salma. S. Abdullah, A. Kadhim and Sabah. A. Salman,” The Fabrication of Cu/Ag, Core/Shell Nanoparticles Dispersed in Various Aqueous Media Using Laser Ablation”, *Academic Science Journal*, Vol.1, pp.130-140, (2023).
- [16] D. Dorranean, E. Solati and L. Dejam, “Photoluminescence of ZnO Nanoparticles Generated by Laser Ablation in Deionized Water”, *Applied Physics A, Materials Science and Processing*, Vol. 109, pp. 307-314, (2012).
- [17] Z. M. Sui, X. Chen, L. M. Xu, W. C. Zhuang, Y. C. Chai and C. J. Yang, “Capping Effect of CTAB on Positively Charged Ag Nanoparticles”, *Physical E*, Vol. 33, pp 308-314, (2006).
- [18] V. Nguyen, L. Yan, J. Si and X. Hou, “Femtosecond Laser Induced Size Reduction of Carbon Nanodots in Solution: Effect of Laser Fluence Spot Size and Irradiation Time”, *Journal of Applied Physics*, Vol. 117, pp. 1-6, (2015).
- [19] M. Rafque, M. S. Rafque, U. Kalsoom, A. Afzal, S, H, Butt, and A. Usman, “Laser Ablation Synthesis of Silver Nanoparticles in Water and Dependence on Laser Nature”, *Optical and Quantum Electronics*, Vol. 51, pp. 1-11, (2019).

